THE TURBULENT INTERSTELLAR MEDIUM: GENERALIZING TO A SCALE-DEPENDENT PHASE CONTINUUM

Colin A. Norman

Department of Physics and Astronomy, Johns Hopkins University

and

Space Telescope Science Institute, Baltimore, MD 21218

Andrea Ferrara

Osservatorio Astrofisico di Arcetri, Largo E. Fermi, 5, 50125 Firenze, Italy

Received _____; accepted _____

ABSTRACT

We discuss the likely sources of turbulence in the ISM and explicitly calculate the detailed grand source function for the conventional sources of turbulence from supernovae, superbubbles, stellar winds and HII regions. We find that the turbulent pumping due to the grand source function is broad band, consequently expanding the inertial range of the cascade. We investigate the general properties of the turbulent spectrum using a simple approach based on a spectral transfer equation derived from the hydrodynamic Kovasznay approximation. There are two major findings in this paper: I. The turbulent pressure calculated from the grand source function is given by $p_{turb} \sim 10 - 100 p_{thermal}$. II. With the scale dependent energy dissipation from a turbulent cascade the multi-phase medium concept can be generalized to a more natural continuum description where density and temperature are functions of scale. Approximate power-law behavior is seen over a large dynamic range. We discuss some of the implications of models for the ISM, particularly addressing the energy balance of the warm neutral phase. However, this paper is not concerned with the detailed structure of the ISM of the Galaxy. Rather, we attempt here to broaden our approach to the global turbulent structure of the ISM and also to move from the current many-phase description to a more natural scale-dependent continuum of phases.

1. INTRODUCTION

Interstellar turbulence in the multi-phase interstellar medium (ISM) has an inertial range stretching over at least 9 orders of magnitude. The substantial viscous and magnetic dissipation at large wavenumbers requires significant energy sources to maintain the spectrum. The evidence for a turbulent spectrum in the multi-phase ISM comes mainly from pulsar observations (Armstrong *et al.* 1981, Rickett 1990, Narayan 1992, Armstrong *et al.* 1995) which are consistent with a cascade from scales of order ~ 100 pc to scales down to 10^{11} cm. Furthermore, the power spectrum appears to be consistent with a Kolmogorov law as reviewed recently by Sridhar and Goldreich (1994). Larson (1981) has also noted a turbulent spectrum in diffuse neutral clouds and molecular clouds. Turbulent pressure plays a crucial role in the various phases of the ISM. This conclusion follows essentially from the work of Kulkarni & Fich (1985) for the cold neutral HI component, and of Reynolds (1985, 1995) for the warm ionized medium. McKee (1990) argued that turbulent pressure has to represent the dominant pressure term in the ISM. Similar conclusions, based on the analysis of the vertical structure of the HI in the Galaxy, were reached independently by Lockman & Gehman (1991) and Ferrara (1993); Boulares & Cox (1990) also recognized the importance of turbulent pressure. There is general agreement on the fact that, following the seminal suggestion by Spitzer (1978), turbulent motion must be associated with energy deposition fromhigh mass stars in the form of winds, HII regions and supernova explosions.

There are a number of outstanding problems with the studies of turbulence in the ISM. It is well known that simple estimates of turbulent dissipation are too high by three orders of magnitude or so (Scheuer 1968, Cesarsky 1980, Spangler 1991, Ferriere *et al.* 1988, Falgarone & Puget 1995). The dissipation problem is intimately related to a Reynolds number that is too low. Using typical numbers from Spangler we find, in general, a Reynolds number of $\mathcal{R} \sim 400$. Furthermore, the associated dynamic range of the cascade

is only $10^2 - 10^5$ which is inconsistent with the observations. The most recent studies of Shridhar & Goldreich (1994), Goldreich & Sridhar (1995) indicate a solution to the previous problems if the spectrum is generated by a magnetized four wave cascade in the wavenumber perpendicular to the field (see also Montgomery & Mattheus 1995; Oughton, Priest & Mattheus 1994; Hossain *et al.* 1995).

Let us now outline the structure of the paper and indicate where to find the principal results. In Section 2 we discuss the general properties of turbulent cascades and their usefulness in understanding the ISM. The mathematical formalism for calculating the turbulent spectrum for a given broad-band source function is presented. We also derive a formula for the turbulent pressure as a function of the grand source function. We derive in Section 3 the grand source function for turbulence in the ISM resulting from supernovae, superbubbles, stellar winds, and HII regions. The properties of the individual source functions are given in Table I. Figure 1 shows the individual contributions to the spectrum and also the total grand source function. The dynamical equations are then solved numerically with the grand source function as input and the results are given in Figure 2. In Section 4 we generalize our analysis to structures called clouds and using the scale-dependent power input from turbulence we are able to calculate the multi-phase properties of an ensemble of turbulently heated clouds. We give a characteristic p-T diagram in Figure 3. In Figures 4 and 5 we indicate how the density and temperature of clouds depends on scale. Section 5 discusses the results of these, albeit idealized, multi-phase calculations and we indicate how they may explain some of the more commonly observed phenomena in the ISM.

2. GENERAL PROPERTIES OF TURBULENT ENERGY CASCADES

In the following we will consider incompressible, homogeneous, isotropic turbulence. This assumption clearly needs some justification when discusssing models appropriate to the multi-phase ISM, which is known to host shock phenomena and highly compressive processes. However, the bulk of our knowledge on turbulence comes from terrestrial laboratory experiments and most of them deal with liquids; in addition one can use those results at least as a reasonable guide when discussing compressible turbulence. In addition, simulations of compressible turbulence (Porter *et al.* 1994) have shown that nonlinear interactions rapidly transfer most of the energy to noncompressible modes.

When dealing with turbulence it is normal to introduce a spectral representation of the velocity field in the fluid. Then, the energy density in eddies with wavenumber between k and $k + dk$ is given by $\rho E(k,t)dk$, where ρ is the density of the fluid and $E(k,t)$ is said to be the (tridimensional) spectrum of the turbulence. Since turbulence is an intrinsically dissipative process, an external source is required in order to maintain a steady spectrum. In the inertial range, however, the dissipation effects can be neglected and the spectrum approaches an universal form that can be derived form general principles using dimensional arguments. *In absence of an external pumping*, the spectrum has the well-known expression $E(k,t) \propto k^{-5/3}$, referred as the Kolmogorov-Obukhoff law. A general approach requires to take into account the equation governing the time evolution of $E(k,t)$, which is called the dynamic equation. In its integral form the dynamic equation reads (Chandrasekhar 1948, Heisenberg 1948, Hinze 1975, Lifschitz & Pitaevskii 1981, Stanisic 1985, Batchelor 1986, Landau & Lifschitz 1987)

$$\frac{\partial}{\partial t}\int_0^k dk' E(k,t) = \int_0^k dk' F(k,t) - 2\nu \int_0^k dk' k^2 E(k,t) + \int_0^k dk' S(k,t); \qquad (2.1)$$

here $F(k,t)$ is the energy-transfer function, ν is the kinematic viscosity and $S(k,t)$ is a source function. The physical meaning of Equation (2.1) is transparent and can be understood in the following way. The LHS term describes the change in the kinetic energy

and the dissipation occurring in large eddies with wavenumber less than k. The flow of energy from large eddies is split in two different contributions: part of it is transmitted in form of kinetic energy to smaller eddies, and part is directly dissipated into heat through viscosity. The first two terms on the RHS describe these two processes, respectively.

A complete solution of the dynamic equation in its general form has not been found yet; the main difficulty is merely a restatement of the *closure* problem for the hydrodynamic equations. In fact, instead of being forced to make an assumption to the next-higher-order velocity correlation, it is necessary here to postulate an explicit form of $F(k,t)$; this is usually done on the basis of some physical/dimensional arguments. A general expression for $F(k,t)$ has been suggested by von Karman (1948) in terms of the interaction function $\mathcal{J}(k',k,t)$:

$$F(k,t) = \int_0^\infty dk \mathcal{J}(k',k,t) = \int_0^k dk' \mathcal{J}(k',k,t) + \int_k^\infty dk'' \mathcal{J}(k'',k,t). \tag{2.2}$$

The interaction function describes the contributions to the eddy with wavenumber k coming from interactions with eddies with $k' < k$ and $k'' > k$; in this sense it has a local character because it does not include the coupling term coming from the interaction of the two modes k' and k'' themselves. According to von Karman, $\mathcal{J}$ can be written as (Hinze 1975, Batchelor 1986, Stanisic 1985)

$$\begin{cases} \mathcal{J}(k',k,t) = 2\alpha E^{3/2-\phi}(k',t) k'^{1/2-\chi} E^{\phi}(k,t) k^{\chi}, & \text{for } k' < k, \quad (2.3a) \\ \mathcal{J}(k,k'',t) = 2\alpha E^{3/2-\phi}(k,t) k^{1/2-\chi} E^{\phi}(k'',t) k''^{\chi}, & \text{for } k'' > k, \quad (2.3b) \end{cases}$$

where α is a numerical constant to be determined from experiments, and the choice of the two exponents ϕ and χ determines the form of the transfer function. Substitution into Equation (2.2), and subsequent integration, give

$$\int_0^k dk F(k,t) = -2\alpha \int_0^k dk' E^{3/2-\phi}(k',t) k'^{1/2-\chi} \int_k^\infty dk'' E^{\phi}(k'',t) k''^{\chi}, \tag{2.4}$$

Probably the most studied choice corresponds to the set $(\phi,\chi) = (1/2, -3/2)$ (Heisenberg 1948); this particular form gives origin to the so-called Heisenberg theory of turbulence, and

the second integral in Equation (2.4) is usually called eddy viscosity. Unfortunately, this choice brings in a strong non-local character which contradicts the hypothesis of statistical independence of the eddies which is at the base of the theory. For that reason, and because this allows an exact analytical solution to be found, we have adopted the formulation proposed by Kovasznay (1948),

$$\int_0^k dk' F(k',t) = -\alpha E^{3/2}(k,t) k^{5/2}, \tag{2.5}$$

which, apart from a numerical constant, corresponds to the case $(\phi, \chi) = (3/2, 0)$. This form automatically satisfies the condition of a local interaction in *every* region of the spectrum. Given the adopted form of the transfer spectrum it follows that Equation (2.1) can be more fruitfully written in its differential form

$$\frac{\partial}{\partial t} E(k,t) = -\alpha \frac{\partial}{\partial k} [E(k,t)^{3/2} k^{5/2}] - 2\nu k^2 E(k,t) + S(k,t). \tag{2.6}$$

The constant α is of the order of unity; for the Heisenberg formulation the correct value extrapolated from the experiments is 0.85 (Hinze 1975), which we have used also for the Kovasznay transfer function.

Equation (2.6) completely describes the evolution of the turbulent spectrum, provided the appropriate boundary and initial conditions

$$\begin{cases} E(0,t) = E(\infty,t) = 0 & 0 \le t < \infty \\ E(k,0) = E_0(k) & 0 \le k < \infty \end{cases} \tag{2.7}$$

are specified.

We will concentrate in the following on steady-state solutions of the dynamic equation.

2.1. Steady-state solutions

The steady state approximation can be used to analyze the physics of the turbulent cascade. We begin by deriving the domain of validity of the steady state assumption. A steady state can be achieved if the eddy turnover time, t_e, is significantly shorter than the interval, t_i, between energy injection events from supernovae, superbubbles, HII regions and winds. For a source rate in the Galaxy $\bar{\gamma}_i$ and a Galaxy volume $V \sim \pi\varpi^2 h$ where h and ϖ are the scale height and the radius of the Galactic disk respectively, the critical ratio of timescales in the interior of the bubble radius R_{0i} is

$$\frac{t_e}{t_i} = \frac{4}{3}\left(\frac{\bar{\gamma}_i R_{0i}^4}{\varpi^2 h v_0}\right) \tag{2.8}$$

where v_0 is the characteristic turbulent velocity on scale R_{0i}.

For supernovae canonical Galactic values (see Table 1) the timescale ratio on scale l is

$$\frac{t_e}{t_i} = 20\left(\frac{l}{R_{0i}}\right)^{\frac{4}{3}}. \tag{2.9}$$

Clearly our steady state assumption is not a very good one close to the injection scale for supernovae and their may be some time dependent effects that can influence the cascade which we will not consider here. However, on scales of order $l \sim 0.1R_{0i}$ the approximation is fair and is increasingly so for larger wavenumbers.

We start writing the steady-state dynamic equation in nondimensional form:

$$\frac{d\Psi_k}{dk} + \mathcal{R}^{-1}k^{1/3}\Psi_k^{2/3} = S(k), \tag{2.10}$$

where $\mathcal{R} = \alpha v_0/2\nu k_0$ is proportional to the Reynolds number corresponding to an dominant eddy of characteristic wavenumber and turnover velocity k_0 and v_0, respectively whose actual values are determined from the input spectrum that we will calculate in this paper. Note that the eddy turnover time is defined as $t_e = 1/(k_0 v_0)$. We have also introduced the

auxiliary variable Ψ_k, such that $E(k) = \Psi_k^{2/3} k^{-5/3}$. For simplicity, we continue to use for the non dimensional variables the same symbols as for the dimensional ones.

To proceed further it is necessary to specify the source function $S(k)$. We will determine the form of this function for various assumptions about the energy injection (supernovae, superbubbles, stellar and galactic winds) in the next Section; here we are interested in finding a solution of Equation (2.10) for a model source function. If, as we are assuming in this paper, turbulent motions in the ISM are induced by interacting blast waves, there are some general constraints on the form of the source function. It is important to emphasize that we are assuming that the observed turbulent motions and the associated inferred turbulent pressure in the ISM are ultimately derived from the kinetic energy of blast waves, winds etc. which, as discussed later, we assume can act as a source function for a turbulent cascade with an efficiency of order unity. We also include reflection from clouds as part of the source function. Bykov & Toptygin (1987) have studied in detail the shock-induced turbulence phenomenon and they find that the turbulent spectrum has, for the McKee & Ostriker (1977) model, a k^{-2} dependence in the short-wavelength regime, while for long wavelengths it is $\propto k^2$. Thus, the simplest source function that retains this behavior is

$$S(k) = \mathcal{S} \frac{k^2}{1 + k^4}. \tag{2.11}$$

In the inertial range, $k_0 \ll k \ll k_d$, where k_d is the dissipation wavenumber, the solution closely approaches the constant value

$$\Psi_k \simeq \frac{\pi}{2\sqrt{2}} \mathcal{S} \simeq \mathcal{S}. \tag{2.12}$$

It follows from Equation (2.12) and from the definition of Ψ_k that

$$E \sim \mathcal{S}^{2/3} k^{-5/3}. \tag{2.13}$$

The energy dissipation rate is given (nondimensionally) by

$$\epsilon_k = \mathcal{R}^{-1} \int_0^k dk k^2 E(k) \simeq \mathcal{R}^{-1} \int_1^k dk k^2 E(k) = \mathcal{R}^{-1} \mathcal{S}^{2/3} k^{4/3} \tag{2.14}$$

where the upper bound dominates.

Thus, the dissipation is an increasing function of the wavenumber. However, the growth must saturate at a k roughly equal to the dissipation wavenumber k_d, to the limiting value $\epsilon_k \simeq \mathcal{S}$. To see this we note that dissipation becomes important when

$$\mathcal{R}^{-1} k^{1/3} \Psi_k^{2/3} \sim \frac{\Psi_k}{k}, \tag{2.15}$$

giving the dissipation wavenumber

$$k_d \sim \Psi_k^{1/4} \mathcal{R}^{3/4} = \mathcal{S}^{1/4} \mathcal{R}^{3/4}. \tag{2.16}$$

When we substitute this expression into Equation (2.14), we find

$$\epsilon_k \simeq \mathcal{R}^{-1} \mathcal{S}^{2/3} (\mathcal{S}^{1/4} \mathcal{R}^{3/4})^{4/3} = \mathcal{S}. \tag{2.17}$$

Of course this result is also a restatement of the steady-state assumption, which implies that the rate of energy dissipation must be equal to the energy injection rate.

The solution Ψ_k remains nearly constant in the entire inertial range up to the dissipation wavenumber k_d. For wavenumbers greater than k_d the dynamic equation is dominated by the dissipative term and can be written as

$$\mathcal{R}^{-1} k^{1/3} \Psi_k^{2/3} \simeq \mathcal{S} k^{-2}. \tag{2.18}$$

which has as a solution

$$\Psi_k = (\mathcal{R}\mathcal{S})^{3/2} k^{-7/2}. \tag{2.19}$$

Note that this corresponds to $E(k) \propto k^{-4}$, for the assumed form of $S(k)$.

If $S(k)$ has a behavior for $k \gg 1$ different from k^{-2}, then the assumption made to obtain Equation (2.12) is no longer valid. The generic source function $S(k) \sim \mathcal{S}k^{-n}$, when the same procedure as in Equation (2.12) is applied, gives the following solutions $\Psi_k^{(n)}$ depending on the value of n

$$\begin{aligned} \Psi_k^{(n<1)} &\sim \mathcal{S}k^{1-n}, \\ \Psi_k^{(n=1)} &= \mathcal{S}\log k, \\ \Psi_k^{(n>1)} &\sim \mathcal{S}. \end{aligned} \tag{2.20}$$

Substituting again into Equation (2.16) we obtain the expressions for k_d:

$$\begin{aligned} k_d^{(n<1)} &\sim \mathcal{R}^{3/(3+n)}\mathcal{S}^{1/(3+n)}, \\ k_d^{(n=1)} &= \mathcal{R}^{3/4}\mathcal{S}^{1/4}(\log k_d)^{1/4}, \\ k_d^{(n>1)} &\sim \mathcal{R}^{3/4}\mathcal{S}^{1/4}. \end{aligned} \tag{2.21}$$

As the previous formulae show, the effect of the pumping is to widen the inertial range beyond the standard value $k_d = \mathcal{R}^{3/4}$ and the gain is proportional to some power of the source term. This suggests that, provided that $\mathcal{S}$ is large enough, the inertial range can extend for several decades. In addition, if $S(k)$ is not too a steep function of k for $k \gg 1$, the effect could be very important: for example, for $n = 0$, the value of k_d is $\mathcal{R}^{1/4}\mathcal{S}^{1/3}$ times larger than its standard value. We refer to this effect as to *broad band pumping* of the turbulence.

An estimate of $\mathcal{S}$ for the various sources can be obtained from dimensional analysis once the expansion law is given. For an expansion law of the source $R \propto t^{\eta}$ the ratio of the

kinetic energy to total energy is, in the thin shell approximation,

$$\frac{K}{E_0} = \left(\frac{\eta}{5\eta - 1}\right). \tag{2.23}$$

It follows, for source i, that $\mathcal{S}_i$ in dimensionless units is

$$\mathcal{S}_i = \left(\frac{\eta}{5\eta - 1}\right) \frac{\gamma_i R_{0i}}{v_0}. \tag{2.24}$$

For supernovae, using the canonical values given in Tab. 1,

$$\mathcal{S}_{SN} \sim 10^5 \left(\frac{\gamma_{SN}}{0.03 \text{ yr}^{-1}}\right) \left(\frac{R_{0SN}}{70 \text{ pc}}\right) \left(\frac{10\text{km s}^{-1}}{v_0}\right). \tag{2.25}$$

2.2 Turbulent Pressure

The pressure due to turbulence is given by

$$p_{turb} = \rho \int_0^\infty dk E(k). \tag{2.26}$$

Using the assumed expression for the source function $S(k)$ as given by Equation (2.11) we integrate Equation (2.26) and find

$$p_{turb} = \rho c_s^2 \mathcal{S}^{2/3} \int_0^\infty dx \; x^{-5/3} \left[\int_0^x dt \frac{t^2}{1+t^4}\right]^{2/3}, \tag{2.27}$$

giving

$$p_{turb} = 6\mathcal{S}^{2/3} p_{th}, \tag{2.28}$$

3. SOURCE FUNCTIONS OF INTERSTELLAR TURBULENCE

There are three catogories for turbulent source functions: (I) shocks from stellar energy input including supernovae, HII regions, winds and superbubbles (Spitzer 1982, Ikeuchi & Spitzer 1984, Bykov & Toptygin 1987); (II) Gravitational sources including spiral waves and bars, tidally driven shocks from interactions, axisymmmetric ($Q \leq 1$) and non-axisymmetric disk instabilities, turbulent wakes from orbiting clouds and general shear-fed instabilities in cool spiral disks (Toomre 1990) and the shear driven by Kelvin-Helmoltz (Balbus 1988) and Balbus-Hawley (Balbus & Hawley 1991 , Hawley & Balbus 1991) instabilities. Note that the Fleck (1982) argument for tapping the shear of the entire gaseous disk is not valid since it violates the Rayleigh criterion; (III) Global flows in the ISM including the global disk-halo circulation (Norman & Ikeuchi 1989), the Parker instability on large scales, and the interaction with infalling high-velocity clouds (Ferrara & Field 1994) or satellites.

We consider in this paper only the conventional sources in category I although it is clear that if the shear of the Galaxy could be efficiently tapped it could dominate the turbulent source functions given here and, therefore, the thermal energy balance of the ISM.

In general, for any source type, i, the mean number of shocks of Mach number μ or greater crossing a given point in the ISM (Bykov & Toptygin 1987) is

$$F_i(\mu) = \frac{4\pi}{3}\gamma_i \frac{R_i^3}{V} \tag{3.1}$$

which, for the self similar solutions given in Table 1, can be written as

$$F_i(\mu) = \frac{4\pi}{3}\frac{R_{0i}^3}{V}\mu^{-\alpha} \tag{3.2}$$

where R_{0i} and α_i are also given in Table 1.

The distribution function $P_i^{(1)}(\mu)$ for primary shocks due to source, i, is

$$P_i^{(1)}(\mu) = -\frac{dF_i}{d\mu} = \frac{4\pi}{3}\alpha_i\gamma_i\frac{R_{0i}^3}{V}\mu^{-(\alpha+1)} = \frac{\alpha_i P_{0i}}{\mu^{(\alpha+1)}} \tag{3.3}$$

where $P_{0i} = \gamma_i V_m/V$, and $V_m = 4\pi/3R_{0i}^3$ is the volume affected by the energy input. Using the same approximation as Bykov & Toptygin (1987) for the secondary shocks, *i.e.,* shocks are reflected off the clouds considered as dense obstacles with volume filling factor f_{cl}, we find

$$P_i^{(2)}(\mu) = \frac{4\pi\alpha_i\gamma_i f_{cl}R_{0i}^3}{(\mu-1)^4 V}C(3;\alpha_i), \tag{3.4}$$

where the coefficient is given by

$$C(n;\alpha_i) = \int_1^{\sqrt{5}}\left(\frac{5-x^2}{3x^2+1}\right)^{(\alpha_i+1)/2}(x-1)^n dx, \tag{3.5}$$

and the relevant numerical values for α_i are given in Table 1.

The resultant shock distribution in the ISM including both primaries and secondaries is

$$P(\mu) = \sum_i P_{0i}\left[\frac{1}{\mu^{\alpha_i+1}} + \frac{3C(3;\alpha_i)f_{cl}}{(\mu-1)^4}\right]. \tag{3.6}$$

The spectrum of the velocity field fluctuations is obtained by assuming a statistically uniform isotropic and stationary ensemble of shocks of a given Mach number μ. By Fourier analyzing the velocity field we find a representation for the spectral energy density distribution, $w_i(k,\mu)$ for source type, i, (se Bykov and Toptygin 1987 for details)

$$w_i = \frac{4c_s^2}{\pi}\frac{(\mu-1)^2k^2R_i^3(\mu)}{\left[1+k^2R^2(\mu)\right]^2}. \tag{3.7}$$

The primary spectrum is obtained by averaging over an ensemble of shocks:

$$S_i^{(1)}(k) = \int_1^\infty w_i(k,\mu) P_{0i}^{(1)}(\mu) d\mu, \tag{3.8}$$

which becomes

$$S_i^{(1)}(k) = c_s^3 \left[\frac{6}{\pi}\right] \beta Q_i (3+\alpha_i) f_i(\alpha_i, k^2 R_{0i}^2). \tag{3.9}$$

We have used the relation $P_{0i} = \gamma_i (V_m/V) = Q_i/t_m$ (where Q_i is the porosity factor for the i-th source), and the parameter $\beta = \eta_i R_{0i}/c_s t_m$, where the maximum radius of the remnant occurs at time t_m (see Cioffi *et al.* 1988); η_i is equal to $\alpha_i/(3+\alpha_i)$. The function f_i can be expressed as a combination of hypergeometric functions:

$$f_i(\alpha_i, k^2 R_{0i}^2) = k^2 R_{0i}^2 \sum_{n=0}^{2} \frac{(-1)^n}{(3-\frac{n}{\delta_i})} F(2, 3-\frac{n}{\delta_i}, 4-\frac{n}{\delta_i}, -k^2 R_{0i}^2). \tag{3.10}$$

with $\delta_i = (2/3)\alpha_i$.

The grand source function is dependent only on γ_i, α_i, and R_{0i}. Canonical values are given in Table 1. Rates have been evaluated using a Salpeter IMF and assuming that the supernova rate for the Galaxy is one every 30 yr due to stars of $8M_\odot$ and above. HII regions are assumed to be formed by stars of $\sim 10 - 20M_\odot$ and above while stellar winds are assumed to be generated by the supernova progenitors.

Following Bykov & Toptygin (1987) we have included one reflection of the primary shocks from clouds in the following next order expression for the source function:

$$S_i(k) = S_i^{(1)}(k) + S_i^{(2)}(k) = c_s^3 \left[\frac{6}{\pi}\right] \beta Q_i (3+\alpha_i) \Big[f_i(\alpha_i, k^2 R_{0i}^2) +$$

$$3f_{cl}\int_1^{\sqrt{5}} d\mu_2 \int_{\mu_2}^{\sqrt{5}} d\mu_0 \left(\frac{5-\mu_0^2}{3\mu_0^2+1}\right)^{(\alpha+1)/2} \left(\frac{\mu_0-1}{\mu_2-1}\right)^3 \frac{\mu_0 0^{\alpha/3}}{\left(\mu_0^{2\alpha/3}+k^2R_{0i}^2\right)}\Big]. \tag{3.11}$$

In evaluating the integral for the reflected shock contribution we have assumed that the integral is dominated by the pole $(\mu_2-1)^{-3}$. The integral over μ_0 is $C(3;\alpha_i)$, and the final approximation of the integral is:

$$S_i^{(2)}(k) = c_s^3\left[\frac{6}{\pi}\right]\beta Q_i(3+\alpha_i)\frac{3f_{cl}}{2}\frac{C(3;\alpha_i)}{\left[1+k^2R_{0i}^2\right]^2\left[\mu_*-1\right]^2}. \tag{3.12}$$

¿From the papers of Spitzer (1982) and Ikeuchi and Spitzer (1984) we note that for Mach numbers $\mu \leq 1.5$ soundwaves are radiated with diminished energy, and for $\mu \leq 2.76$ no reflected shock waves are found. Conservatively we cut-off μ at $\mu_* = 1.5$. A good estimate for the reflected component of the turbulence is then

$$S_i^{(2)}(k) = c_s^3\left[\frac{6}{\pi}\right]\beta Q_i(3+\alpha_i)6f_{cl}\frac{C(3;\alpha_i)}{[1+k^2R_{0i}^2)]^2}. \tag{3.13}$$

The individual source functions S_i are reported in Fig. 1 along with the grand one. We note that the latter is strongly dominated by supernovae and therefore the grand source function closely resembles the simple one used for the analytical solution (Equation 2.10) above: the approximation $S(k) \propto k^{-2}$ is excellent in the entire inertial regime. Although the rates γ_i are similar for the different sources since they originate from stars of comparable mass, the α values are different. Since the integrand is a steep function of α_i, the smallest α_i values tend to dominate and for this reason supernovae and superbubbles the major contributors to the grand source function. However, the region close to the maximum of S_i is broader than the one expected from Equation (2.11). In fact superbubbles are dominant becuse of their steep $\alpha = 9/2$ in contrast to the $\alpha = 9/7$ of the SNe. Consequently, superbubbles deposit approximately the same energy as supernovae over a much narrower range of wavenumbers thus dominating on those scales.

Secondary shocks contribute sensibly only for small k, while their importance is marginal in the inertial regime. The value of $\mathcal{S}$ inferred from Fig. 1 is $\mathcal{S} \sim 50$; then from Equation (2.28), $p_{turb} \sim 80 p_{th}$, in agreement with the resulti obtained integrating numerically on the grand source function. In Fig. 2 we give the numerical solution of the dynamic equation (2.11) using the source function calculated above. Where a canonical number for the Reynold's number is necessary we have used a value of 10^5 using standard values for the viscosity following Scalo (1987).

4. TURBULENT THERMAL BALANCE

In the previous Section we have demonstrated that the dissipation rate up to a wavenumber k is $\epsilon_k = \mathcal{R}^{-1}\mathcal{S}^{2/3}k^{4/3}$. This implies that *the energy input is scale-dependent*. We now follow Larson (1981) and generalize our thinking and analysis to a set of structures and velocites on different scales that forms part of a general energy cascade. This is not a rigorous step but physically it is most interesting since it allows us to analyse multi-phase media with a reasonable scale-dependent energy input. In other words, we can study the ISM as a set of structures on different scales characterized by a specific thermal balance between turbulent heating and standard cooling. We show that multi-phase equilibria may exist for a wide range of conditions. For want of a better name we call these structures clouds but they are, following Larson (1981), clouds, clumps, subclumps, cores etc.

We first investigate under which conditions turbulent dissipation can support the various of the ISM. For simplicity, we ignore other important heating processes such as photoelectric effects from grains (Wolfire et al 1995) and focus on the structure that emerges with turbulent dissipative heating. The temperature for a cloud of wavenumber T_k can be obtained from the energy balance equation, which is obtained by equating radiative

energy losses with turbulent heating to give

$$2\rho\nu \int_0^k dk k^2 E(k) = n_e^2 \Lambda(T), \tag{4.1}$$

where $n_e^2\Lambda(T)$ is the cooling rate per unit volume (see Appendix A), n_e is the electron density, ρ is the mass density of the gas. Because of the difficulties of understanding the presence of the large inertial range of the turbulence observed in the ISM, due to the small inertial range that is nominally calculated from standard viscosity values (Ferriere *et al.* 1988, Spangler 1991) we have chosen to parametrize our collective ignorance in the Reynolds number. Therefore we can rewrite Equation (4.1) as

$$\frac{2\rho v_0}{k_0 \mathcal{R}} \int_0^k dk k^2 E(k) = n_e^2 \Lambda(T). \tag{4.2}$$

where k_0 and v_0 are derived form the spectrum. A further simplification that allows an equation for the temperature only to be derived is that the pressure of the ISM is fixed at $\tilde{p} = nT$. Multi-phase structure is usually analysed in p-T diagrams (Field 1965; Field, Goldsmith & Habing 1969; Dalgarno & McCray 1972). However, since in general the net cooling function depends both on T and x, the ionization fraction, at low temperatures the thermal balance equation must be solved together with the ionization equation. We will assume that ionization in the ISM is mainly governed by cosmic-rays (X-ray ionization would give similar results); also, we will neglect their contribution to the heating with respect to the turbulent one. The details of the calculation below are given in Appendix A.

To derive the phase diagrams we now use Equation (2.13) as an accurate approximation for $E(k)$; we also use Equation (2.16) as an expression for k_d. Then Equation (4.2) can be written

$$\tilde{p} = \frac{T^2}{\Lambda(T)} \left[\frac{3}{2} \left(\frac{k_B \mathcal{S}}{t_e} \right) \left(\frac{k}{k_d} \right)^{4/3} \right], \tag{4.3}$$

where t_e is defined in Sec. 2.1. For $\mathcal{S} \sim 100$ and $t_e \sim 10^{12}$ s then

$$\tilde{p} = 2 \times 10^{-26} \frac{T^2}{\Lambda(T)} \left(\frac{k}{k_d} \right)^{4/3}.$$

For $k \sim k_d$, the $\tilde{p} - T$ relation is plotted in Fig. 3. It is clear then that at the dissipation scale only the very dense, cold phase can absorb the power and be the dissipative sink. Our conclusion is in contrast to Ferriere *et al.* (1988), who attempted to use the less dense warm neutral medium as the preferential dissipative site. They concluded correctly that the energy balance for the warm neutral medium failed by several orders of magnitude. However, as we shall show, the dissipation problem is solved by incorporating scale dependent energy dissipation that follows naturally from the turbulent cascade. In this case the temperature of the multiphase medium that results is a function of scale. The density spectrum is also a function of wavenumber.

To see this we fix the thermal pressure at a fiducial value $\tilde{p} = 3000 \tilde{p}_{3000}$ cm^{-3} K. Then we directly infer from Equation (4.3) that

$$\left(\frac{k}{k_d} \right) = 7.6 \times 10^{21} \left[\frac{\Lambda(T)}{T^2} \right]^{3/4}. \tag{4.4}$$

The corresponding $T - k$ relation is shown in Fig. 4. We also derive the density spectrum directly from Fig. 4 using $n = \tilde{p}/T$, and this is shown in Fig. 5. For $\mathcal{S} \simeq 100$ and $\mathcal{R} = 10^5$, we have $k_d = \mathcal{S}^{1/4} \mathcal{R}^{3/4} \simeq 10^4 \mathcal{S}_2^{1/4} \mathcal{R}_5^{3/4}$. The relevant range of interest for the parameters used in this paper is $10^{-4} \leq (k/k_d) \leq 1$.

The phase diagrams of our admittedly basic model of the turbulent and turbulently heated ISM plotted in Figs. 4-5 could represent a generalization albeit of previous work

on multi-phase models of the ISM. The number of phases required to explain the ISM has been increasing with time. Our results exhibit a natural extension to a *continuum* of phases in pressure equilibrium, where both the temperature and density of the ISM are continuous functions of scale. From an inspection of Figs. 4-5 it is clear that cold, dense gas is preferentially found on small scales, while the warmer, less dense material is only at equilibrium on much larger scales. Obviously, approximate power-laws can be fit to the density curve and in Fig. 5, over the range of interest, we find $n \sim (k/k_d)^{.55}$. This shows the approximately fractal nature of the continuous phase structure in a turbulently heated medium; the corresponding fractal dimension is $d = 2.45$.

We note the following caveat represented by the possible onset of thermal instabilities in some temperature ranges (Field 1965; Corbelli & Ferrara 1995). This would complicate the thermal structure of the gas considerably: in particular, some parts of the phase continuum shown in the phase diagrams may split in two (or more) separate branches, increasing the overall complexity of the system. The detailed form of this branching may depend on nonlinear feedback processes that regulate the pressure of the ISM and that are qualitatively introduced and briefly discussed in Sec. 5.

5. SUMMARY AND CONCLUSIONS

We have discussed the physics and mathematical description of the turbulent energy cascade in the ISM (Section 2). The grand source function for turbulent energy sources has been derived including the contribution of conventional sources as supernovae, superbubbles, stellar winds, and HII regions (Section 3). The results are shown in Figure 1 and the properties of the individual source functions are given in Table I. Supernovae dominate over most of the spectral range although superbubbles can dominate on large scales. We find

that the turbulent pumping due to the grand source function is broad band, consequently expanding the inertial range of the cascade. The dynamical equations are solved and the results presented in Figure 2. The turbulent pressure calculated from the grand source function (Section 2.2) is given by $p_{turb} \sim 10 - 100 p_{thermal}$. With the scale dependent energy dissipation from a turbulent cascade the multi-phase medium concept becomes a continuum description where density and temperature are functions of scale (Section 4). Approximate fractal behavior is seen over a large dynamic range. The thermal properties of the ISM on the large scales are similar to the conventional models. On smaller scales turbulent heating can dominate and a multi-phase structure can develop for the hydrodynamic cascade discussed here. A typical p-T diagram is presented in Figure 3. The derived temperature and density of clouds in this multi-phase structure are functions of the scale of the observing measurement and might be regarded as an approximate fractal. Typical results exhibiting this behaviour are given in Figures 4 and 5.

We have ignored various potentially important feedback effects in this paper, regarding them as important to incorporate in the next stage of calculational complexity. For example, when we use the grand source function in the calculation of the phase diagram there are temperature dependences hidden in the R_{0i}'s that may create potential feedback effects on the phase diagram structure shown in Figs. 3, 4, and 5. Such feedback effects will be discussed in a subsequent paper.

This is a steady state calculation with no consideration given to the initial conditions and how the system can evolve to the steady state. In fact, it may be difficult for the system to reach this state. If the temperature is less than the temperature associated with the maximum of the cooling curve that a substantial fraction of the gas must go over, then the hot phase will never be formed. If for other physical reasons the hot phase is formed then the equilibrium state can be maintained. The two-equilibrium temperatures are actually

two foci in the phase-plane $T - \dot{T}$ of the time-dependent equation. The essential point is that the regions of attraction of the two foci are such that the system will remain attracted to the lower equilibrium temperature unless it is put over the hump of the cooling curve and can be attracted to the higher equilibrium temperature. The condition for this is exactly as described above.

A further complication arises when a magnetized turbulent cascade is utilized. This is a necessary ingredient since the ISM is certainly magnetized. The spectrum found is similar to a Kolmogorov spectrum but is highly anisotropic and is a Kolmogorov spectrum in the wave-number perpendicular to the magnetic field i.e. $E_M(k_\perp) \sim k_\perp^{-5/3}$ (Shridhar & Goldreich 1994, Goldreich & Shridhar 1995,Oughton, Priest and Mattheus 1994, Montgomery & Mattheus 1995). As discussed in detail by Ferriere *et al.* (1988), Spangler (1991), and Goldreich & Shridhar (1995), Alfvén waves in the cascade will propagate without damping in the very highly ionized ISM but will dissipate rapidly on the edges of clouds consistent with the qualitative discussion in this paper. However, the details of the dissipative processes need further study and clarification since there seems to be a significant discrepancy between the observed inertial range of the turbulence of up to 10 orders of magnitude and the rather high dissipation rates inferred for the standard ISM.

The source of the turbulent pressure that holds up the ISM against its own weight is clearly evident in our analysis with the principal being energy input form massive stars via supernova remnants and superbubbles. The spectrum of the predicted velocity has been presented and it may be possible to constrain our results by observations of large scale turbulence via measurements of the large scale velocity fields (HI, Hα, IR fine cooling fine structure lines, recombination lines). As we shall discuss in a later paper, many other heat sources come into play in the ISM (Wolfire *et al.* 1995) including direct shock heating from supernovae and superbubbles, photoelectric heating from grains, soft X-ray heating etc.

(Wolfire *et al.* 1995). Many of these heat sources are scale-dependent. Therefore, the range of validity of turbulent heating effects for our Galaxy may be limited to the cooler material.

The scale-dependent phase continuum model of the ISM presented here may be a beginning of a more useful description of the ISM than the current many-phase models particularly for the understanding and integration of the many detailed observations of the ISM.

We thank the Aspen Center for Physics, Arcetri Observatory, ESO Garching, and the Institute of Astronomy, Cambridge whose stimulating environments, hospitality and support are gratefully acknowledged. We particularly thank R. Bandiera, T. Heckman, P. Pietrini, Yu. Shchekinov, J. Slavin, and M. Spaans for valuable comments.

APPENDIX A.

Here we briefly outline the assumptions made in the calculation of the cooling functions. More details can be found in Ferrara & Field (1994). We have adopted the "on the spot" approximation in which diffuse field photons are supposed to be absorbed close to the point where they have been generated. The various elements are divided into "primary" ones, which enter the ionization-thermal equilibrium and "secondary"ones which do not. In the following, H is considered as primary, while other elements (He, C, N, O, Si, Fe) just contribute to the cooling function. Secondary elements, apart from He, are considered to be completely ionized by the UV field below 13.6 eV; a helium abundance equal to 0.1 H as been assumed. Double ionization of He has been neglected, and He fractional ionization has been supposed equal to the H one, x. The following processes have been included in the calculation of the cooling function $\Lambda(x, T)$: i) free-free emission; ii) H and He recombination; iii) electron impact ionization of H and He; iv) electron impact excitation of H and He (n=2,3,4 triplets); v) He dielectronic recombination; vi) electron and H impact excitation of

secondary elements; excitation of the metastable levels by electron impact are also included. The cooling function obtained is shown in Fig. 2. by Dalgarno & McCray (1972) for the range $T \lesssim 10^4$ K. At higher temperature the cooling curve has been calculated using the radiation code by Landini & Monsignori-Fossi (1990).

The ionization fraction is calculated as follows. Assume that the energy density in cosmic rays is proportional to the thermal pressure in the Galaxy. Normalizing to canonical values for the Galaxy we find the ionization rate

$$\xi = n_{cr}\sigma c \simeq 3 \times 10^{-16}\tilde{p}_{3000}, \qquad (A1)$$

where σ is the low-energy cosmic-ray cross section, c is the speed of light. We can write the ionization equation as

$$n^2 x^2 \alpha(T) = (1-x)n\xi, \qquad (A2)$$

and using Equation (A1) we find

$$x^2 \frac{\alpha(T)}{T} = (1-x)\xi_0, \qquad (A3)$$

with $\xi_0 = 3 \times 10^{-19}$ s^{-1}, and $\alpha(T)$ is the radiative recombination coefficient; Equation (A3) gives the dependence of x on T.

APPENDIX B.

In Table 1 we have defined the following symbols and relations:

$$R_{SN} = 14.0 \frac{E_{51}^{\frac{2}{7}}}{n_0^{\frac{3}{7}} \zeta_m^{\frac{1}{7}}} \text{ pc},$$

$$\tau_{SN} = 3.61 \times 10^4 \frac{E_{51}^{\frac{3}{14}}}{n_0^{\frac{4}{7}} \zeta_m^{\frac{5}{14}}} \text{ yr},$$

where E_{51} is the energy of a supernova in units of 10^{51} erg, ζ_m and n_0 are the metallicity and the average density of the gas respectively (Cioffi *et al.* 1988). R_S is the Stromgren radius of the star forming the HII region under consideration. The sound speed in the neutral and ionized media are given by $C_I = c_s$ and C_{II}, respectively. L and L_{SB} are the luminosities of winds and superbubbles, respectively.

REFERENCES

Armstrong, J.W., Cordes, J.M., and Rickett, B.J. 1981, Nature 291, 561

Armstrong, J.W., Rickett, B.J. and Spangler, S.R. 1995 ApJ 443, 209

Balbus, S. 1988, ApJ 324, 60

Balbus, S. & Hawley, S. A. 1991, ApJ 376, 214

Batchelor, G. K. 1986, The Theory of Homogeneous turbulence, (Cambridge: Univ. Press)

Boulares, A. & Cox, D. P, 1990, ApJ, 365, 544

Bykov, A. N. & Toptygin, I. N. 1987, ApSS, 138, 341

Cesarsky, C. 1980, ARA&A, 18, 289

Chandrasekhar, S. 1949, Phys. Rev., 75, 896

Cioffi, D., McKee, C.F. & Bertschiger, E. 1988, ApJ 334, 252

Corbelli, E. & Ferrara, A. 1995, ApJ, 447, 708

Dalgarno, A. & McCray, R. 1972, ARA&A, 10, 375

Falgarone, E. & Puget, J.-L. 1995, A&A, in press

Ferrara, A. 1993, ApJ, 407, 157

Ferrara, A. & Field, G. B. 1994, ApJ, 423, 665

Ferriere, K., Zweibel, E. & Shull, M. 1988, ApJ 332, 984

Field, G. B. 1965, ApJ, 142, 531

Field, G. B., Goldsmith, D. W. & Habing, H. J. 1969, ApJ, 155, L149

Fleck, C. 1982, ApJ 261, 631

Goldreich, P. & Sridhar, S. 1995, ApJ 438, 763

Hawley, S. & Balbus, S. 1991, ApJ 376, 223

Heiles, C. 1987, ApJ 315, 555

Heisenberg, W. 1948, Proc. Roy. Soc. London, A, 195, 402

Hinze, J. O. 1975, Turbulence, (New York:McGraw-Hill)

Hossain, M., Gray, P.C., Pontius, D.H., Mattheus, W.H., Oughton, S. 1995, Phys. Fluids, in press.

Ikeuchi, S. & Spitzer, L. 1984, ApJ283, 825

Kovasznay, L. S. G. 1948, J. Aeronaut. Sci., 15, 745

Kulkarni S. R. & Fich, M. 1985, ApJ, 289, 792

Landau, L. D. & Lifshitz, E. M. 1987, Fluid Mechanics, (Oxford:Pergamon)

Landini, M & Monsignori Fossi, B. C. 1990, AASS, 82, 229

Larson, R. 1981, MNRAS 194, 809

Lifshitz, E. M. & Pitaevskii, L. P. 1981, Physical Kinetics, (Oxford:Pergamon)

Lockman, F. J. & Gehman, C. S. 1991, ApJ, 382, 182

McKee, C. F. & Ostriker, J. P. 1977, ApJ, 218, 148 (MO)

McKee, C. F. in "The Evolution of the Interstellar Medium", PASP Conf. Series, ed. L. Blitz, (San Francisco:ASP), 3

Montgomery, D. & Mattheus, W.H. 1995, ApJ 407, 706

Narayan, R. 1992, Phyl. Tran. R. Soc. London A, 341, 151

Norman, C. & Ikeuchi, S. 1989, ApJ 345, 372

Oughton, S., Priest, E.R. and Mattheus, W.H. 1994, J. Fluid Mech. 280, 95.

Porter, D. H., Pouquet, A. & Woodward, P. R. 1994, Phys Fluids A, in press

Reynolds, R. J. 1985, ApJ, 294, 256

Reynolds, R. J. 1995, in The Physics of the Interstellar Medium and of Intergalactic Medium, PASP Conf. Series, Vol. 80, eds. A. Ferrara, C. F. Mc Kee, C. Heiles, P. R. Shapiro, (San Francisco:ASP), 388

Rickett, B. J. 1990, ARA&A, 28, 561

Scheuer, P.A.G. 1968, Nature 218, 920

Scalo, J. M. 1987, in Interstellar Processes, eds. D.J. Hollenbach & H. A. Thronson, 349

Spangler, S. R. 1991, ApJ, 376, 540

Spitzer, L. 1978, Physical Processes in the Interstellar Medium, (New York: Wiley)

Spitzer, L. 1982, ApJ 262, 315

Sridhar, S. & Goldreich, P. 1994, ApJ, 432, 612

Stanisic, M. M. 1985, The Mathematical Theory of Turbulence, (New York: Springer-Verlag)

Toomre, A. 1990 in Dynamics and Interaction of Galaxies, ed. R.Wielen, (New York: Springer-Verlag), p. 272

von Karman, T. 1948, Proc. Natl. Acad. Sci. U.S., 34, 530

Wolfire, M.G., Hollenbach, D., McKee, C.F., Tielens, A.G.G.N. and Bakes, E.L.O. 1995, ApJ 443, 152.

This manuscript was prepared with the AAS LaTeX macros v3.0.

Fig. 1.— Normalized turbulent source functions $S_i(k)$ for supernovae, superbubbles, winds and HII regions. *Solid lines* show the sum of primary and secondary shock contributions for each source; *dashed lines* show secondary shocks only. The thick line is the total grand source function.

TABLE 1. SOURCE FUNCTIONS FOR TURBULENCE IN THE ISM *

	SUPERNOVAE	HII REGIONS	WINDS	SUPERBUBBLES
Expansion Law	$R = R_{SN}\left[\frac{4te}{3\tau_{SN}} - \frac{1}{3}\right]^{\frac{3}{10}}$	$R = R_{HII}\left[1 + \frac{7C_{II}t}{4R_{HII}}\right]^{\frac{4}{7}}$	$R = \left[\frac{L}{\rho}\right]^{\frac{1}{5}} t^{\frac{3}{5}}$	$R = \left[\frac{125L_{SB}}{154\pi\rho}\right]^{\frac{1}{5}} t^{\frac{3}{5}}$
$R - \mu$ relation	$R = R_{0SN}\mu^{-\frac{2}{3}}$	$R = R_{0HII}\mu^{-\frac{4}{3}}$	$R = R_{0W}\mu^{-\frac{3}{2}}$	$R = R_{0SB}\mu^{-\frac{3}{2}}$
R_{0i}	$R_{SN}\left[\frac{2R_{SN}}{5c_s\tau_{SN}}\right]^{\frac{3}{7}}$	$\left[\frac{7C_{II}}{4C_I}\right]^{\frac{4}{3}} R_S$	$\left[\frac{27L}{125\rho c_s^3}\right]^{\frac{1}{2}}$	$\left[\frac{27L_{SB}}{154\pi\rho c_s^3}\right]^{\frac{1}{2}}$
α_i	9/7	4	9/2	9/2
CANONICAL VALUES				
γ_i (yr)	1/30	1/60	1/30	1/3000
R_{0i} (pc)	70	30	70	1000

* See Appendix B for definition of various quantities

Fig. 2.— Solution of the steady-state dynamic equation, $\psi_k^{2/3}k^{5/3}$, for Reynolds number $\mathcal{R} = 10^5$ as a function of wavenumber, using the grand source function shown in Fig. 1. The spectrum $E(k) = \psi_k^{2/3}k^{5/3}$ is also shown together with the dissipation rate ϵ_k.

Fig. 3.— Pressure - temperature relation at $k = k_d$ for pumping number $\mathcal{S} \sim 100$, Reynolds number $\mathcal{R} = 10^5$, and eddy turnover time $t_e = 3 \times 10^4$ yr.

Fig. 4.— Temperature as a function of wavenumber for pumping number $\mathcal{S} \sim 100$, Reynolds number $\mathcal{R} = 10^5$, and eddy turnover time $t_e = 3 \times 10^4$ yr. The continuum structure is almost fractal in major portions of the diagram.

Fig. 5.— Density spectrum as a function of wavenumber for pumping number $\mathcal{S} \sim 100$, Reynolds number $\mathcal{R} = 10^5$, and eddy turnover time $t_e = 3 \times 10^4$ yr. In the range $-5 \leq log(k/k_d) \leq 0$, the approximate density power index is 0.55, again exhibiting approximate fractal behavior over a large dynamic range.

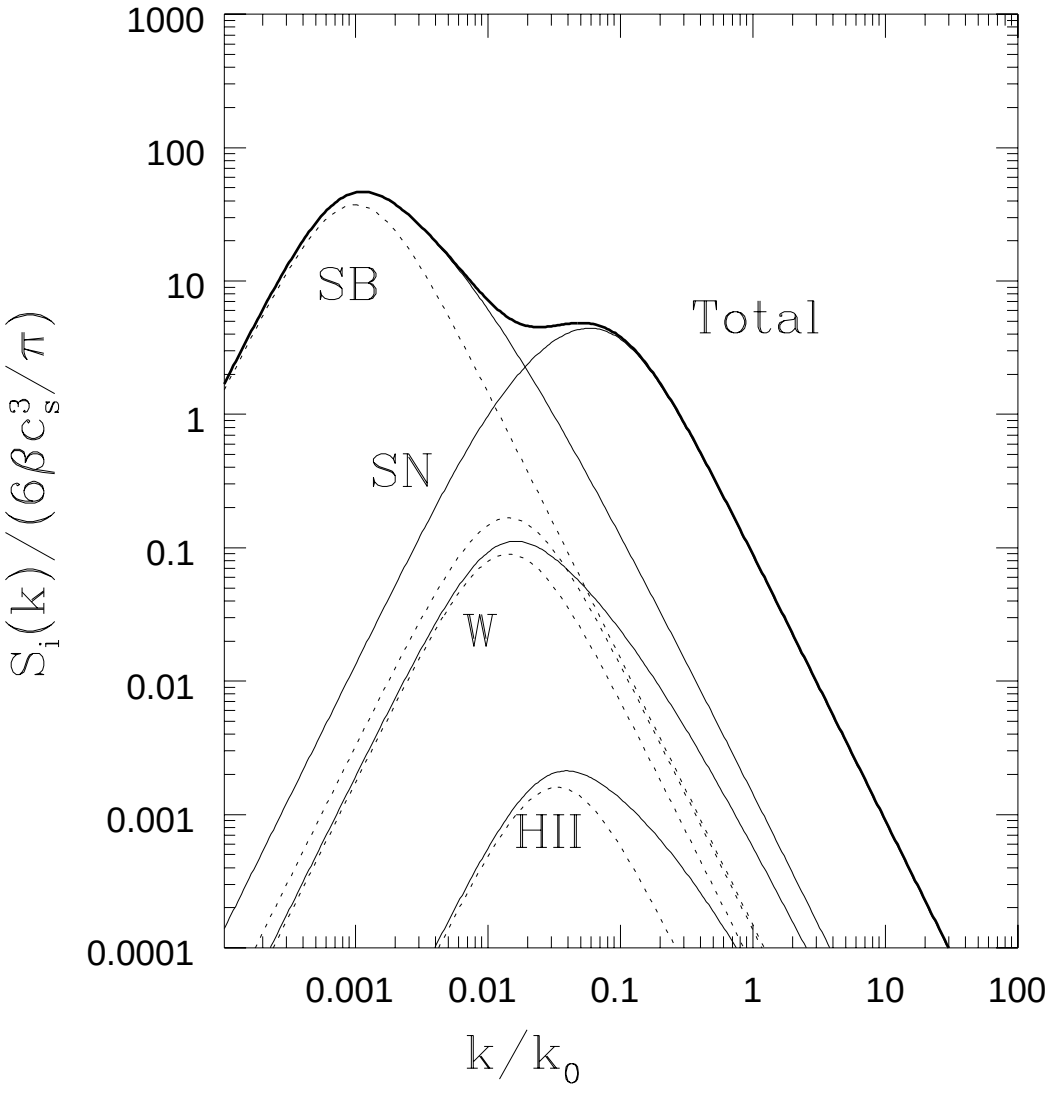
1000
100
10
1
0.1
0.01
0.001
0.0001
0.001
0.01
0.1
1
10
100
SB
Total
SN
W
HII
$S_i(k)/(6\beta c_s^3/\pi)$
k/k_0

Fig. 1

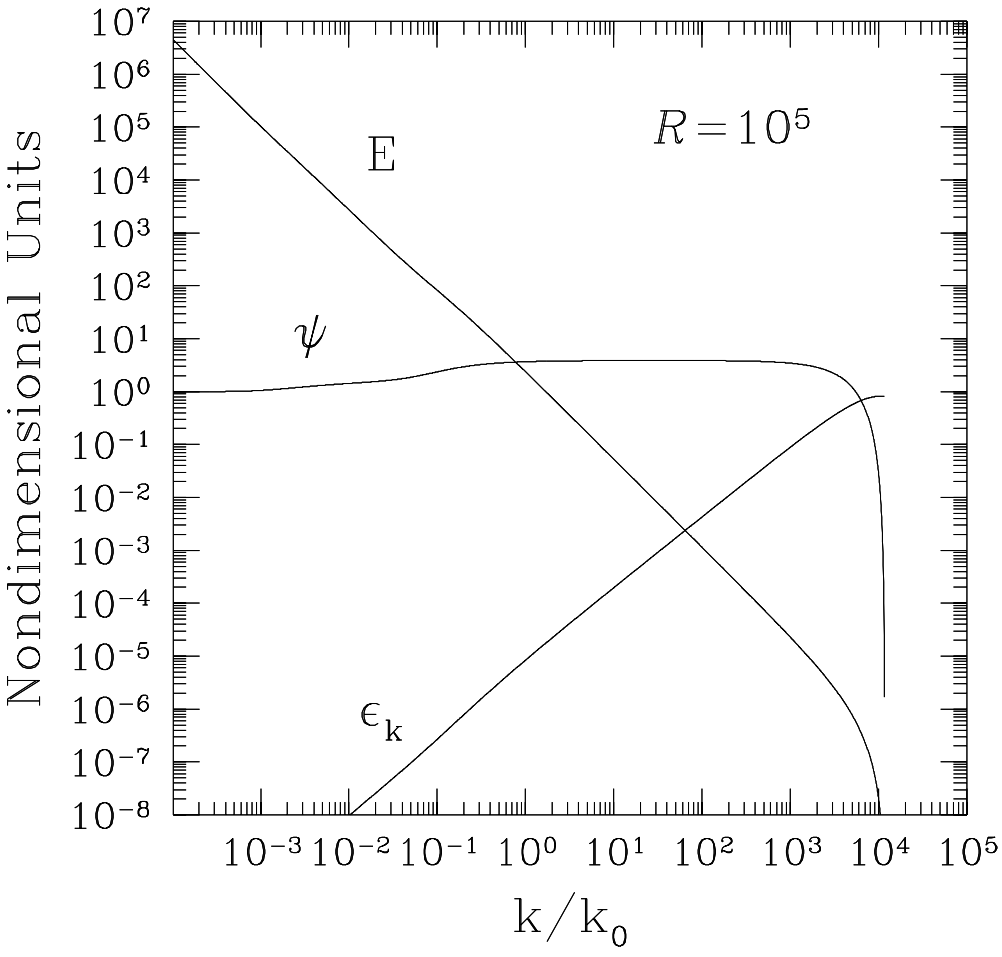
Nondimensional Units
10^{7}
10^{6}
10^{5}
10^{4}
10^{3}
10^{2}
10^{1}
10^{0}
10^{-1}
10^{-2}
10^{-3}
10^{-4}
10^{-5}
10^{-6}
10^{-7}
10^{-8}
$R = 10^{5}$
E
ψ
ϵ_k
10^{-3} 10^{-2} 10^{-1} 10^{0} 10^{1} 10^{2} 10^{3} 10^{4} 10^{5}
k/k_0

Fig. 2

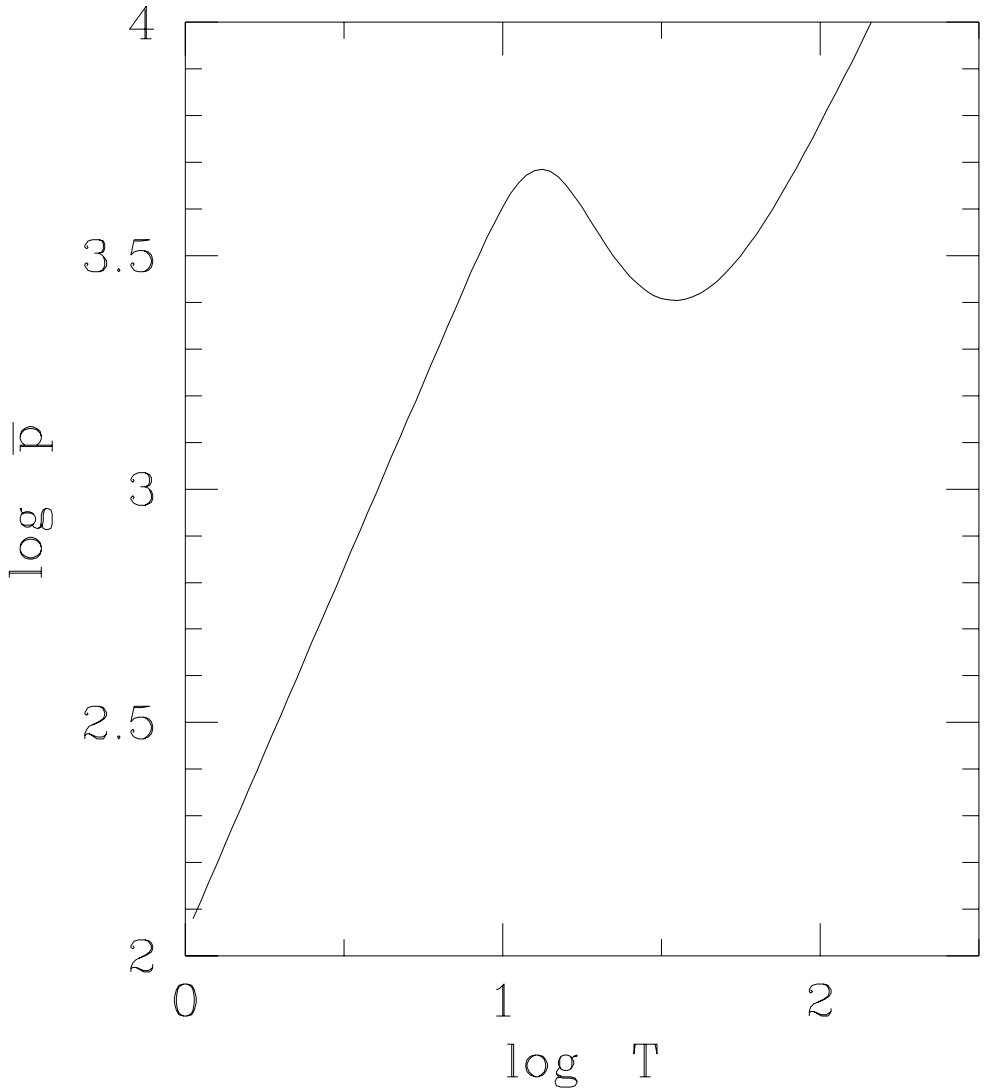

Fig. 3